Preliminary Tests of a Precision VHF Omnirange

By

Sterling R Anderson
Robert B Flint
William L Wright
and
John Turk

Electronics Division

TECHNICAL DEVELOPMENT REPORT NO. 355

CIVIL AERONAUTICS ADMINISTRATION
TECHNICAL DEVELOPMENT CENTER
INDIANAPOLIS, INDIANA

August 1958

U S. DEPARTMENT OF COMMERCE
Sinclair Weeks, Secretary

CIVIL AERONAUTICS ADMINISTRATION
James T Pyle, Administrator
D M. Stuart, Director, Technical Development Center

TABLE OF CONTENTS

	Page
SUMMARY	1
INTRODUCTION	1
THEORY	2
EQUIPMENT DESCRIPTION AND CALIBRATION	9
FLIGHT TESTS	9
CONCLUSIONS	17

This is a technical information report and does not necessarily represent CAA policy in all respects

PRELIMINARY TESTS OF A PRECISION VHF OMNIRANGE*

SUMMARY

This report presents the theory and results of the preliminary development and testing of a new precision VHF omnirange in which omnibearing information is produced by radiating, in effect, a rotating 10-lobe radio-frequency sideband pattern in contrast to the rotating 2-lobe pattern of a conventional omnirange Theoretically, a 5 to 1 improvement is possible in bearing accuracy and a substantial reduction of course scalloping caused by reflecting objects can be effected

An experimental model of the precision omnirange, using 21 loops, was installed at the CAA Technical Development Center, Indianapolis, Indiana The measured bearing accuracy was plus or minus 0 35°. The maximum course scalloping caused by reflections from a horizontal wire 200 feet in length and 30 feet high was 30 6 per cent of the scalloping associated with a conventional 4-loop omnirange at the same site Later, measurements of course scalloping caused by reflections from groups of trees were made at a decommissioned five-loop omnirange site at Dayton, Ohio, using the same experimental equipment The maximum course scalloping at this site was the same for both antenna systems, however, the azimuthal area of scalloping on the precision omnirange was only 27 4 per cent of the area of scalloping on the 5-loop omnirange On radial flights, a reduction in course bends varying from 2 to 1 to 6 to 1 was measured on the precision omnirange Polarization errors measured in flight were negligible

INTRODUCTION

Finding suitable omnirange sites sometimes is a difficult problem because buildings, wires, fences, trees, and so forth reflect the electromagnetic waves radiated from the omnirange to cause various bearing errors, termed "siting errors." These errors appear as course scalloping, course roughness, course bends, and in special cases, fixed errors Specifications for siting the VOR (VHF omnirange) have been established which are a compromise between the ideal site and that which may be available Accordingly, many VOR sites are far from ideal and, occasionally, siting errors are introduced, notwithstanding the inherent excellence of the VOR antenna and associated equipment.

It has been known for a number of years that a multilobe omnirange (more than two lobes in the rotating pattern) should possess certain advantages in reducing siting errors The multilobe omnirange, however, possesses ambiguities that must be resolved by some other means

The idea for a precision omnirange was conceived at the Technical Development Center (TDC) in 1954, and a theoretical study was started in July 1955 With the objective of determining the reduction of siting error possible from a multilobe omnirange as well as determining the inherent bearing accuracy, a precision omnirange was designed and built. Tests were begun in 1956 at this Center The results were so encouraging that arrangements were made with the CAA First Regional Office of Air Navigation Facilities to test the precision omnirange at a wooded site near Dayton, Ohio This site previously was found wholly unacceptable as a Regional VOR facility The tests at the Dayton, Ohio, site were conducted during September and October, 1957

This report describes the theory and the preliminary development of the experimental precision omnirange and discusses the results of tests conducted at Indianapolis, Indiana, and Dayton, Ohio, which were concerned primarily with scalloping and siting effects Methods of resolving the inherent ambiguity of bearings were not investigated, although several solutions are possible

---

*Manuscript submitted for publication May 1958

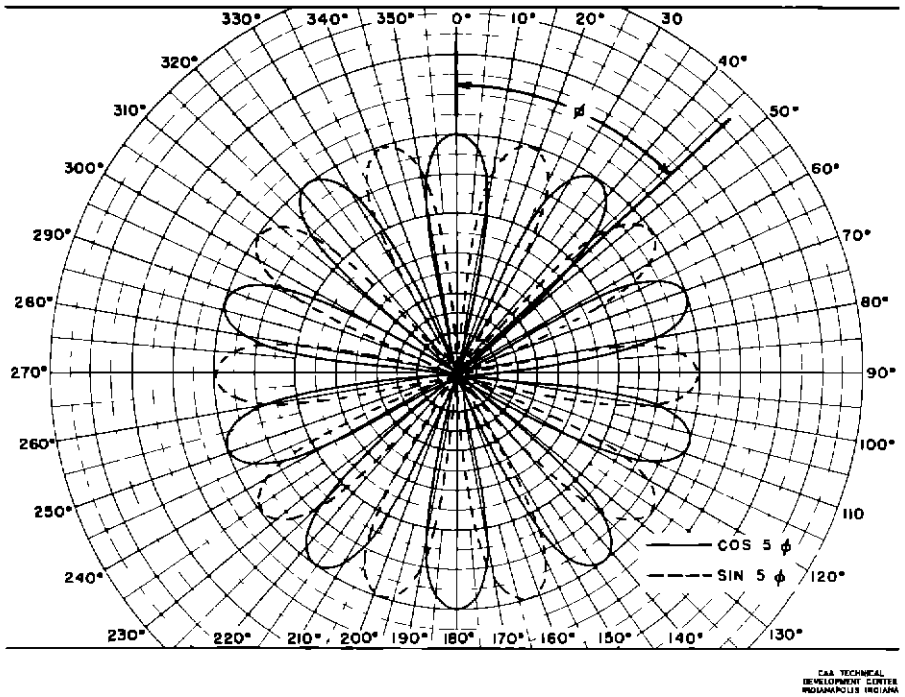

Fig 1 Horizontal Plane Patterns of the Sideband Radiations (Approximate)

THEORY

General

Assume 20 loops, equally spaced on the circumference of a circle 1 wavelength (8.56 feet) in radius Ten of the loops, spaced 36° apart, radiate a cos 5 ϕ pattern and the alternate 10 loops radiate a sin 5 ϕ pattern The horizontal plane patterns of the 20-loop radiators are shown in Fig 1 The outputs of a conventional VOR goniometer feed sideband energy to the 2 sets of 10 loops This may be expressed mathematically

e_1 = goniometer No 1 output voltage = $E_m \sin \rho t \cos \omega t$ (1)

e_2 = goniometer No 2 output voltage = $E_m \sin \rho t \sin \omega t$ (2)

where

E_m = constant voltage

$\frac{\rho}{2\pi}$ = radio frequency (that is, 115 Mc)

$\frac{\omega}{2\pi}$ = audio frequency (that is, 30 cps)

t = time

The voltage e_1 drives the set of 10 loops producing the cos 5 ϕ horizontal plane pattern and, therefore, the signal radiated at azimuth ϕ is

$F_1 = E_m \sin \rho t \cos \omega t \cos 5\phi$ (3)

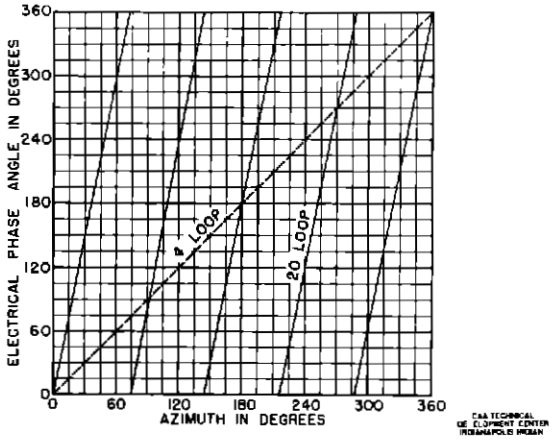

Fig 2 Electrical Phase Angle Versus the Azimuth Angle for the 20-Loop and 4-Loop Omniranges

and the signal at azimuth ϕ radiated by the 10 loops producing pattern sin 5 ϕ when energized by e_2 becomes

$$F_2 = E_m \sin \rho t \sin \omega t \sin 5\phi. \tag{4}$$

The total signal received in direction ϕ is

$$F = F_1 + F_2 = E_m \sin \rho t \cos (\omega t - 5\phi) \tag{5}$$

Equation (5) represents a sideband signal containing an audio frequency $\frac{\omega}{2\pi}$ whose phase angle varies as the azimuth angle multiplied by 5 The phase angle 5 ϕ is measured in the aircraft receiver. Ambiguities in the 5 ϕ information can be resolved by observing the azimuth from the conventional VOR A study of Fig 2 shows that any given electrical phase angle of the precision system corresponds to 5 azimuth angles For example, 180° electrical phase angle is associated with azimuth angles 36°, 108°, 180°, 252°, and 324° The slope of the curves for the precision omnirange is five times as great as the slope of the curve for the conventional VOR This accounts for the greater precision of the new omnirange

Derivation of the Horizontal Plane Field Patterns

So far, it has been shown that a precision omnirange is possible where a change of azimuth of 1° will result in a change in electrical phase angle of 5°. To accomplish this, it is required that a horizontal plane pattern that follows a sin 5 ϕ or cos 5 ϕ function be produced as shown in Fig 1 An antenna array producing such a pattern was discovered mathematically Figure 3 shows a plan view of two antennas, A and B, at ϕ_1, r, and (ϕ_1 + 180°), r, respectively The currents in the antennas are of equal amplitude, but the phase angles are reversed. The sum of the fields radiated by the two antennas in a direction ϕ at a great distance R may be expressed as

$$E = 1\, e^{+j\alpha_1} e^{-j\left[KR - Kr\cos(\phi - \phi_1)\right]} + 1\, e^{-j\alpha_1} e^{-j\left[KR + Kr\cos(\phi - \phi_1)\right]} \tag{6}$$

where

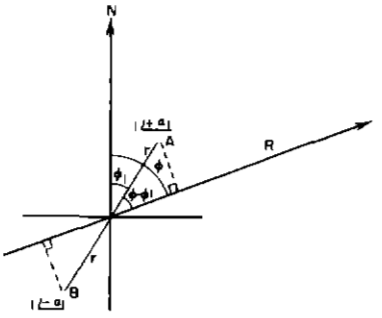

Fig 3 A Plan View Showing Two Antennas of the Precision Omnirange

$$K = \frac{2\pi}{\lambda}$$

λ = wavelength

α_1 = r-f phase angle of antenna currents.

By trigonometry

$$E = 2\, e^{-jKR} \cos\left[\alpha_1 + Kr\, \cos(\phi - \phi_1)\right] \tag{7}$$

In the following, the term $2\, e^{-jKR}$ is omitted since it is constant with azimuth A number of pairs of antennas may be added to the first pair, all located on one circle of radius r with the resulting expression

$$E = \Big\{ \cos\left[\alpha_1 + Kr\, \cos(\phi - \phi_1)\right] + \cos\left[\alpha_2 + Kr\, \cos(\phi - \phi_2)\right] + \cos\left[\alpha_3 + Kr\, \cos(\phi - \phi_3)\right] + \cos\left[\alpha_4 + Kr\, \cos(\phi - \phi_4)\right] + \ldots \Big\} \tag{8}$$

The 20-loop array tested at this Center consisted of two groups, of 10 loops each, arranged in a circle of 8 56 feet radius The sin 5 ϕ loops were positioned at intervals of 36°, while the cos 5 ϕ loops were positioned midway between the sin 5 ϕ loops as shown on Fig 4

Equation (8) with $\alpha_1 = \alpha_3 = \alpha_5 = +90°$, $\alpha_2 = \alpha_4 = -90°$, $K_r = 360°$, $\phi_1 = 18°$, $\phi_2 = 54°$, $\phi_3 = 90°$, $\phi_4 = 126°$, and $\phi_5 = 162°$ becomes

$$E = \Big\{ + \sin\left[360° \cos(\phi - 18°)\right] - \sin\left[360° \cos(\phi - 54°)\right] + \sin\left[360° \cos(\phi - 90°)\right] - \sin\left[360° \cos(\phi - 126°)\right] + \sin\left[360° \cos(\phi - 162°)\right] \tag{9}$$

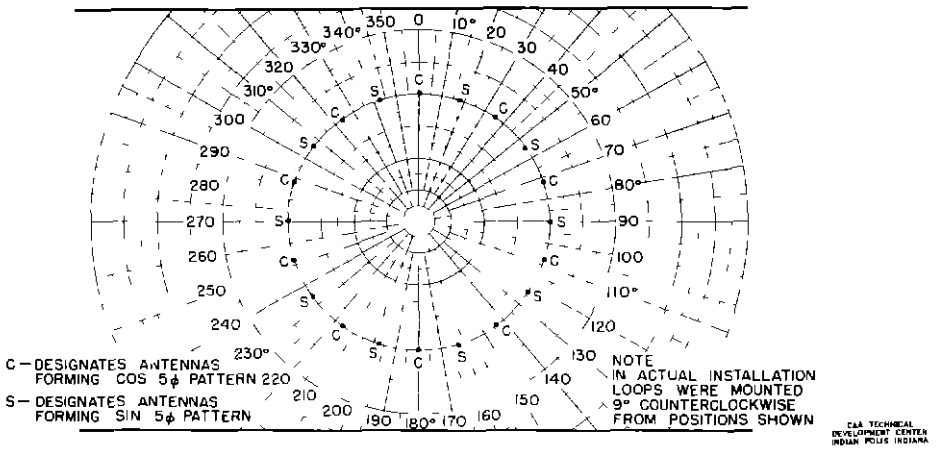

Fig 4 A Plan View Showing the Location of the Antennas on the 2λ Diameter Circle

Equation (9) is worked out for 0° to 18° azimuth and a comparison is made with the values of sin 5 ϕ in Table I and Fig 5. Figure 5 represents one-half of the dashed lobe of Fig 1 which extends from 0° to 36° Because of symmetry, Fig 5 may be thought to represent all parts of the two patterns shown on Fig 1 The significance of the close agreement between the desired field pattern and the 10-element array field pattern means that small bearing errors may be expected to result in practice, where a 5 to 1 correspondence between electrical degrees and azimuthal degrees is assumed

Course Scalloping

The course scalloping to be expected on the precision omnirange may be derived in the same way as for a conventional[1] VOR Figure 6 shows the situation where T is the omnirange transmitting antenna, R is a reflecting object which is assumed to have a non-directional pattern of radiation, and P is the omnirange receiver in an aircraft at an azimuth of ϕ from the omnirange The direct wave from an omnirange with n equal sectors of 360 electrical degrees each may be expressed as

$$E_o = \frac{e^{-jKr_o}}{r_o} \qquad \left[1 + \cos(\omega t - n\phi)\right] \tag{10}$$

and the wave from the reflecting object located at $\phi = 90°$ is

$$E_1 = \frac{A\, e^{-j(Kr_1 + \delta)}}{r_1} \qquad \left[1 + \cos(\omega t - 90° n)\right] \tag{11}$$

where

A = electric field intensity at the aircraft of the wave traveling along r_1 divided by the electric field intensity at the aircraft of the wave traveling along r_o

δ = phase change of the r-f electric field intensity due to reflection

[1] S R Anderson and H F Keary, "VHF Omnirange Wave Reflections from Wires," CAA Technical Development Report No 126, May 1952, Fig. 6

TABLE I

A COMPARISON BETWEEN DESIRED FIELD STRENGTH, COLUMN (1), AND COLUMN (2), THE FIELD STRENGTH FROM EQUATION (9)

ϕ (degrees)	(1) sin 5 ϕ	(2) $\frac{E}{3\,723}$
0	0	0
2	.1736	1757
4	3420	.3433
6	5000	4993
8	6428	.6401
10	7660	7636
12	8660	8668
14	9397	9377
16	9848	9852
18	1 0000	1 0000

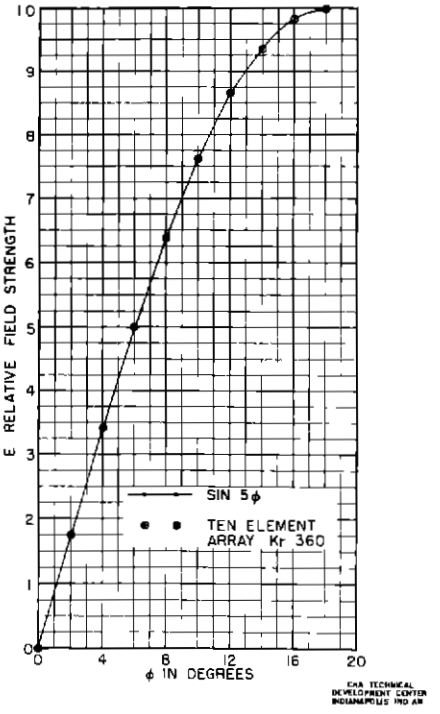

Fig 5 A Comparison Between The Desired Horizontal Plane Pattern and the Ten-Element Theoretical Array Pattern

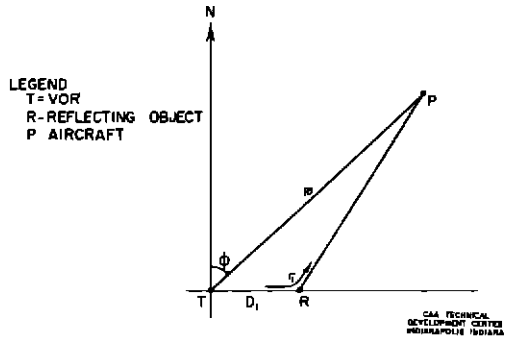

Fig 6 A Plan View Showing the Omnirange Transmitter, Reflecting Object, and Aircraft

The reflected and direct waves combine at point P

$$E = E_o + E_1 \tag{12}$$

Equation (12) may be expressed as a carrier with $\frac{\omega}{2\pi}$ sidebands correctly phased with the carrier in order to produce an amplitude modulated wave. The phase angle of the modulation frequency becomes

$$B = \tan^{-1}\left\{\frac{\cos\zeta \sin n\phi + A \sin(90°n)\cos\left[K(r_1 - r_o) + \delta + \zeta\right]}{\cos\zeta \cos n\phi + A\cos(90°n)\cos\left[K(r_1 - r_o) + \delta + \zeta\right]}\right\} \tag{13}$$

where

$$\zeta = -\tan^{-1}\left\{\frac{A \sin K(r_1 - r_o) + \delta}{1 + A\cos\left[K(r_1 - r_o) + \delta\right]}\right\} \tag{14}$$

The error in the phase angle B is the amount it differs from the value of B with no reflection present If A = 0 in equation (13), then

$$B = n\phi \tag{15}$$

Bearing error expressed in electrical degrees, caused by the reflecting object (course scalloping), is

$$\Omega_n = B - n\phi = \tan^{-1}\left\{\frac{\cos\zeta \sin n\phi + A \sin(90°n)\cos\left[K(r_1 - r_o) + \delta + \zeta\right]}{\cos\zeta \cos n\phi + A\cos(90°n)\cos\left[K(r_1 - r_o) + \delta + \zeta\right]}\right\} - n\phi \tag{16}$$

When equation (16) is to express error in terms of degrees of azimuth rather than electrical degrees, the electrical degrees must be divided by n

With the conditions, $\cos\zeta \approx 1$, $A \leq 0.1$, and n = 1, equation (16) becomes

$$\Omega_1 = \tan^{-1}\tan\phi + \frac{A\cos\left[K(r_1 - r_o) + \delta + \zeta\right]}{\cos\phi} - \phi \tag{17}$$

When n = 5

$$\Omega_5 = \frac{1}{5}\tan^{-1}\left\{\tan 5\phi + \frac{A\cos\left[K(r_1 - r_o) + \delta + \zeta\right]}{\cos 5\phi}\right\} - \phi \tag{18}$$

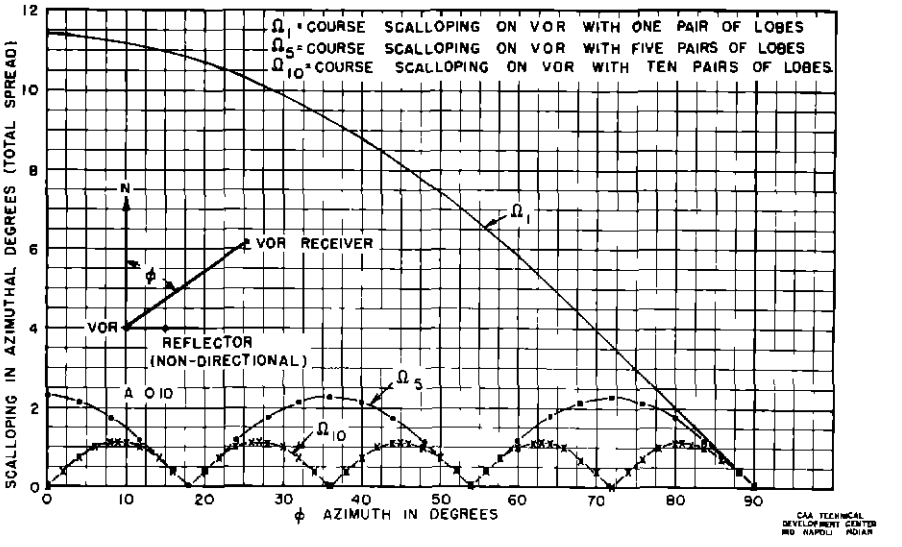

Fig 7 Course Scalloping Caused by One Reflecting Object Versus Azimuth

When n = 10

$$\Omega_{10} = \frac{1}{10} \tan^{-1} \left\{ \frac{\sin 10\,\phi}{\cos 10\,\phi - A \cos \left[K(r_1 - r_o) + \delta + \zeta\right]} \right\} - \phi \qquad (19)$$

Equations (17), (18), and (19) each have a term, $\cos \left[K(r_1 - r_o) + \delta + \zeta\right]$ which varies from a plus 1 to a minus 1 with aircraft motion Since approximate maximum plus and minus bearing errors are desired, this term may be replaced with plus or minus 1 Also, equations (17), (18), and (19) may be simplified to the following forms

$$\Omega_1 = \tan^{-1} \left(\frac{\cos \phi}{\sin \phi \pm \frac{1}{A}} \right) \qquad (20)$$

$$\Omega_5 = \frac{1}{5} \tan^{-1} \left(\frac{\cos 5\,\phi}{\sin 5\,\phi \pm \frac{1}{A}} \right) \qquad (21)$$

$$\Omega_{10} = \frac{1}{10} \tan^{-1} \left(\frac{\sin 10\,\phi}{\cos 10\,\phi \pm \frac{1}{A}} \right) \qquad (22)$$

Figure 7 shows plots of equations (20), (21), and (22) for one quadrant It will be noted that in the approximate sector 70° to 90°, the scalloping or bearing error caused by the reflector to a 1-pair type omnirange is reduced only little by replacing it with a 5-pair type omnirange In tests comparing the 1-pair system and the 5-pair system, little improvement was noted However, since the 10-pair system places a null at $\phi = 72°$, as shown in Fig 7, a marked improvement can be expected by replacing the 5-pair system with the 10-pair system where the reflecting object is of such a kind as to make the scalloping in this sector important

Figure 8 contains the data of Fig 7, presented in terms of the scalloping associated with the conventional VOR, a one-pair system, in order to show the amount of improvement theoretically possible from the two precision omniranges under study Referring to Fig 8, in the sector from approximately 80° to 90°, little improvement is obtained from the 5-pair system over the 1-pair system The figure makes clear that in this sector, a 10-pair system is considerably more effective in reducing scalloping

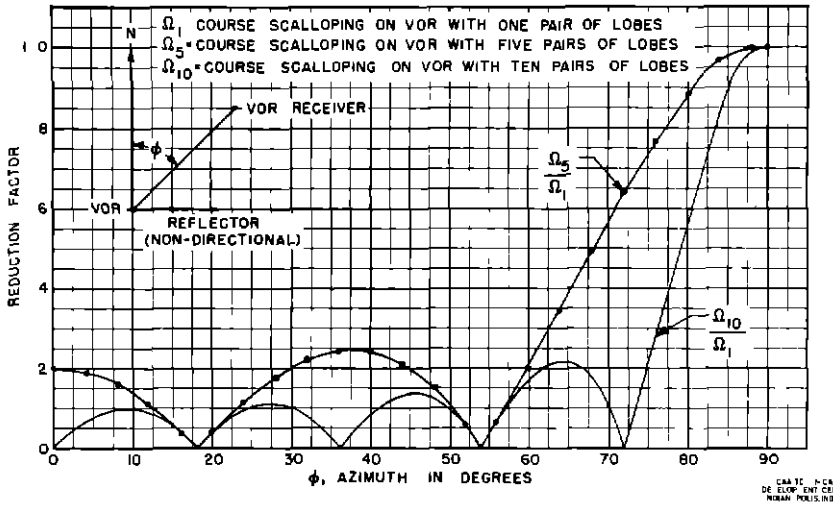

Fig 8 Reduction in Course Scalloping Effected by the Precision Omnirange Compared with a Conventional VOR

EQUIPMENT DESCRIPTION AND CALIBRATION

The experimental precision VOR consisted of conventional VOR equipment, but with the conventional 4-loop antenna and transmission lines replaced with a single carrier loop and 20 sideband loops and associated r-f lines The 20 sideband loops were mounted on the counterpoise on a circle having a radius of 8 56 feet and at intervals of 18°, or 32 16 inches between centers The No 1 loop was located at 351°, the No 2 loop at 9°, and so forth. Loops Nos. 1 and 2 were connected for clockwise rotation, Nos 3 and 4 for counterclockwise rotation, and so on for each pair of loops. The loops were connected to the VOR goniometer outputs as illustrated in Fig 9 The goniometer speed was 1,800 rpm, as in a conventional VOR. Junction boxes shown in Figs 10A and 10B were used for paralleling the ten r-f lines of each sideband group

The installation of the precision VOR at the north range site at TDC is shown in Fig 11 The loops were protected from weather by covers fabricated from polyethylene sheeting The counterpoise was 10 feet high and 35 feet in diameter The procedure for adjusting the precision VOR was similar to that used for adjusting a conventional VOR

The ground calibration measurements[2] were made with a VOR monitor field detector at a radius of 200 feet from the station, at 4° azimuth intervals (20 electrical degrees) Measuring equipment included a Type CA-1277 VOR monitor, a Type CA-1430 VOR reference and variable test generator, and a Type 2559 DuMont oscilloscope A plot of the ground calibration of the precision VOR is shown in Fig 12 The maximum bearing error was plus or minus 0.35°.

FLIGHT TESTS

Flight tests were conducted at Indianapolis to determine the amount of course scalloping as compared to the scalloping measured previously on a conventional VOR at the same site

A Collins Type 51R3 navigation receiver and an Esterline-Angus graphic recorder were used for recording in flight the course deviation indicator (CDI) current The indicator circuit of the precision VOR receiver was adjusted for one-fifth normal course sensitivity so that the recording of the CDI current would show the same course deviation in degrees

---

[2] Robert B Flint and William L Wright, "Ground Calibration of the VOR," CAA Technical Development Report No 227, October 1955

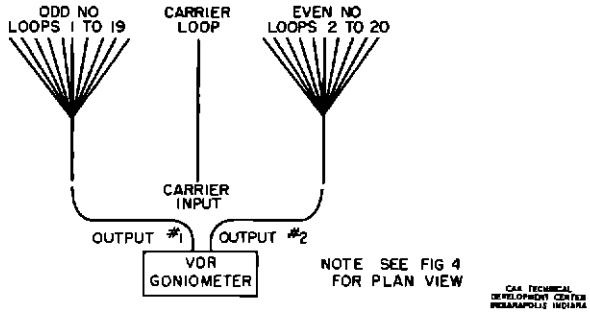

Fig 9 Diagram Illustrating Method of Exciting the 20-Loop Antennas of the Precision VOR

of azimuth as would be recorded normally on a conventional VOR The omnibearing selector (OBS) was modified to include a second resolver unit which rotated 5 revolutions for 1 revolution of the standard OBS resolver Thus, the flight engineer used the same procedure for recording the precision VOR as for the conventional VOR

Course scalloping was determined by recording the CDI current at an altitude of 1,000 feet above ground at a distance of 15 miles from the VOR A plot of the course scalloping caused by a horizontal No 6 copper wire, 200 feet long, suspended between 30-foot masts at a distance of 177 feet from the VOR, is shown in Fig 13. This test simulated tests made previously with a four-loop VOR [3] The maximum course scalloping from the 4-loop VOR was plus or minus 2.45° compared to plus or minus 0 75° for the precision VOR A comparison of the scalloping areas shows a 19 to 1 reduction for the precision omnirange

Siting tests were made with both a four-loop VOR and the precision VOR mounted on the counterpoise. Course scalloping was measured on the 4-loop VOR, then on the precision VOR, as the aircraft circled the station at a radius of 20 miles at 1,000 feet above ground A comparison of the course scalloping for the two antenna systems is shown in Fig 14. These data also are plotted in polar coordinates in Fig 15 The principal reflecting objects are shown in Fig 15 The maximum course scalloping on the 4-loop VOR was plus or minus 1 5° compared to plus or minus 0 85° on the precision VOR A comparison of the scalloping areas shows a 10 to 1 reduction for the precision omnirange

On completion of the flight tests at Indianapolis, it was decided to make a temporary installation of the precision VOR at the site of a decommissioned five-loop omnirange at Dayton, Ohio The five-loop VOR at this site had been plagued with course scalloping and bending in excess of the allowable limits due to trees The installation of the precision VOR at the Dayton, Ohio, VOR is shown in Fig 16 This counterpoise is 30 feet high and 35 feet in diameter A map of the site is shown in Fig 17, and an aerial view is shown in Fig 18 The maximum course scalloping was caused by the wooded section, shown in Fig. 16, 825 feet south of the VOR. Considerable course scalloping also was caused by the small woods 1,500 feet northwest of the VOR Figure 19 is a view of the woods to the northwest of the site

Polar diagrams of the course scalloping plotted from the recordings of the CDI current obtained during flights at a 20-mile radius for the precision VOR and the 5-loop VOR are shown in Fig 20 The maximum course scalloping from both VOR's was plus or minus 2.3°. The scalloping area for the 5-loop VOR was 3 65 times as large as the area for the precision VOR It will be observed that the course scalloping for the precision VOR is confined fairly well to the direction of the wooded sectors

Radial flights were made at an altitude of 6,000 feet above ground and to distances of 40 miles from the VOR Recordings of the CDI current for both the precision and five-loop VOR's are shown in Figs 21, 22, 23, and 24 These recordings were mechanically re-recorded from the original recordings, so that 8 feet of the original recording is compressed into 1 foot For each pair of radial recordings, the course deviation was considerably less for the precision VOR than for the five-loop VOR A large error generally occurred at the first null in the vertical plane radiation pattern at 9 5 miles from the station for both systems.

---

[3] Anderson and Keary, op. cit , pp 16-17.

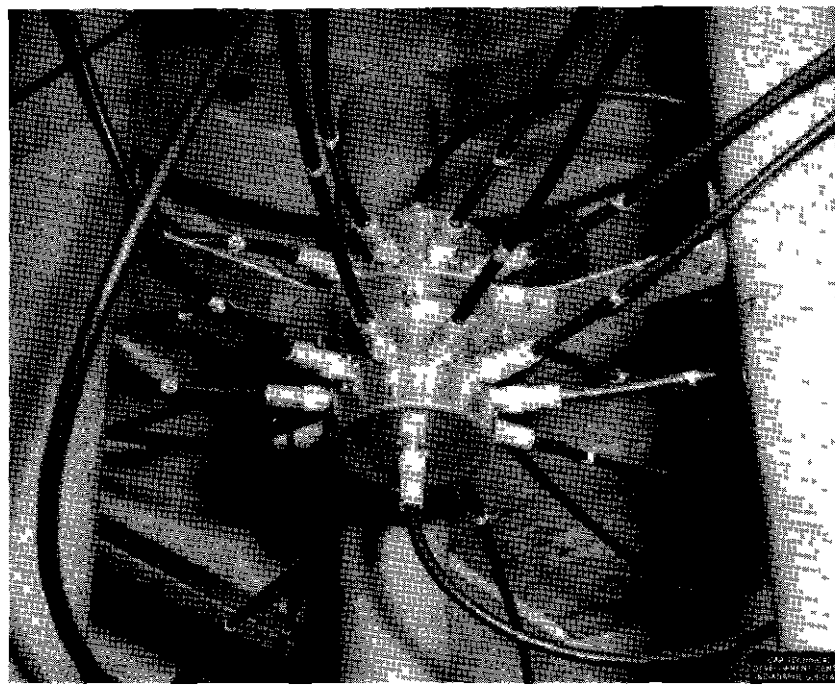

Fig 10A Junction Boxes for Paralleling R-F Lines

Fig 10B Inside View of Junction Boxes for Paralleling R-F Lines

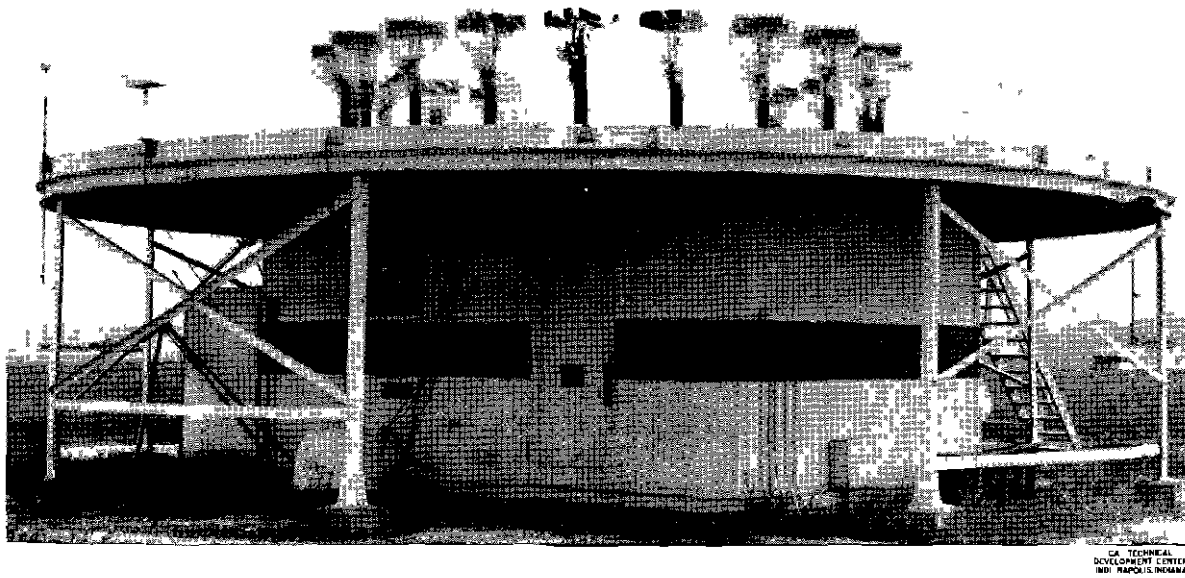

Fig 11 Precision VOR Installation at TDC

Radial recordings of the precision VOR were comparatively free of large course deviations at distances beyond 12 miles from the station, while the radial recordings from the 5-loop VOR show large excursions of the course deviation indicator at all distances Polarization error on the precision VOR during radial flights was negligible

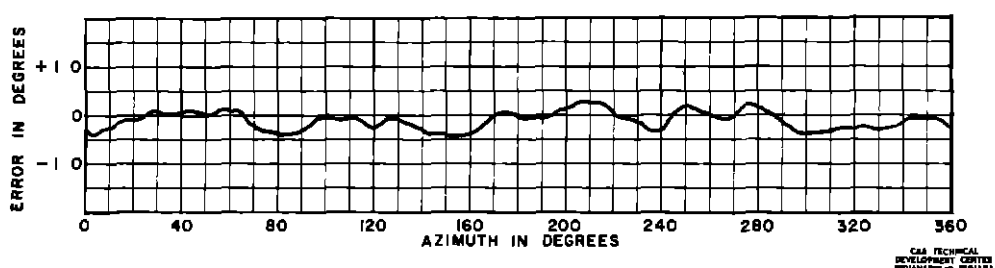

Fig 12 Ground Calibration of the Precision VOR

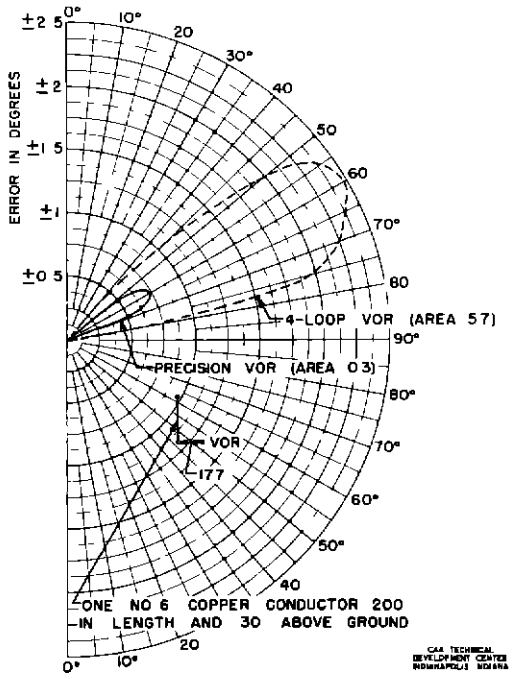

Fig 13 Polar Plot of Course Scalloping with a Horizontal Wire as the Reflecting Object

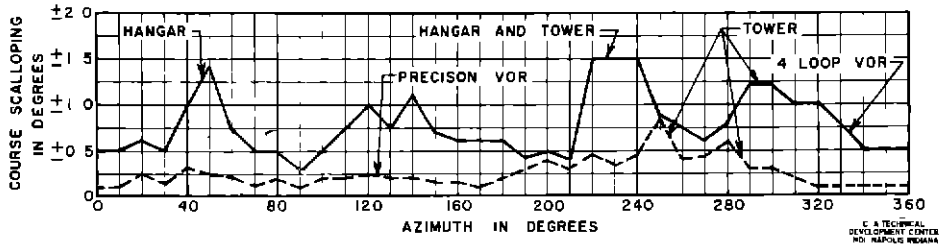

Fig 14 Rectangular Plot of Course Scalloping for the TDC Installation of the Four-Loop VOR and the Precision VOR

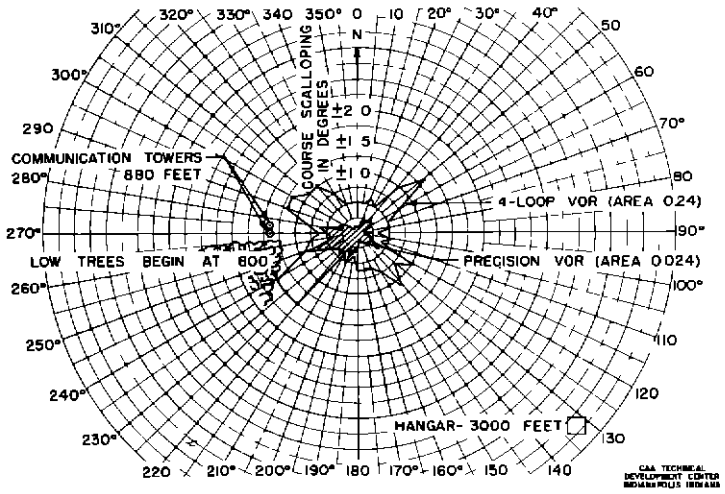

Fig 15 Polar Plot of Course Scalloping for the TDC Installation of the Four-Loop VOR and the Precision VOR

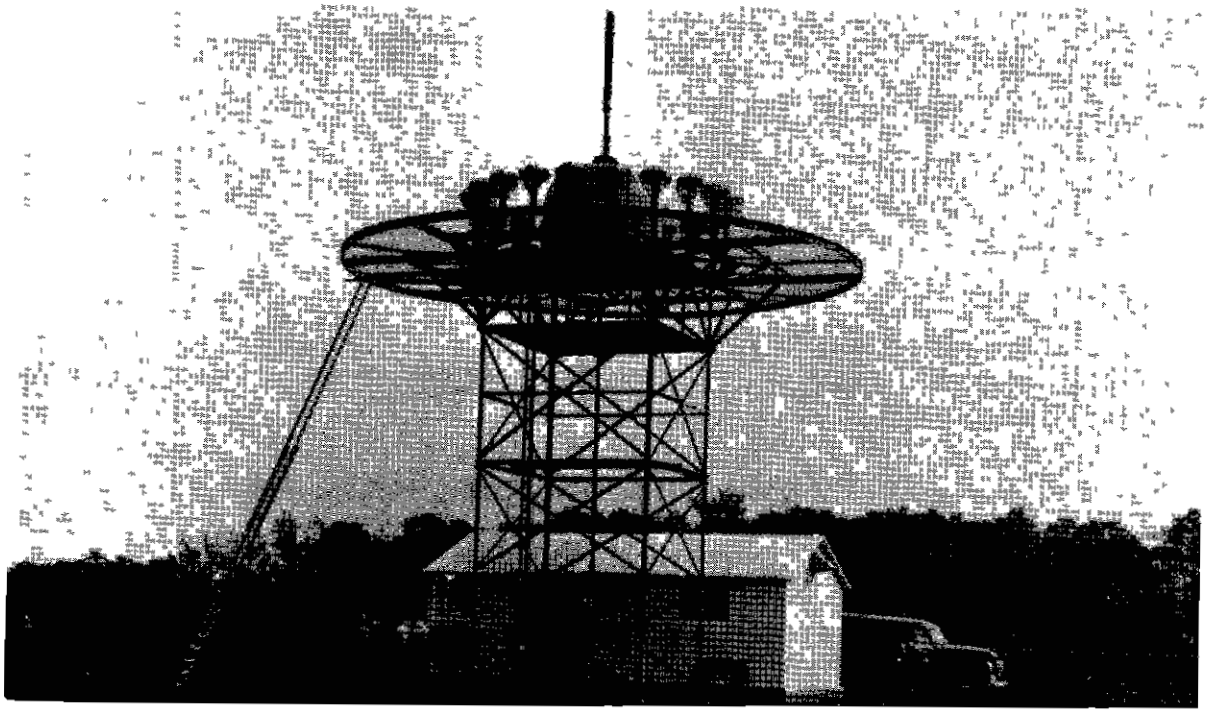

Fig 16 Precision VOR Installation at Dayton, Ohio

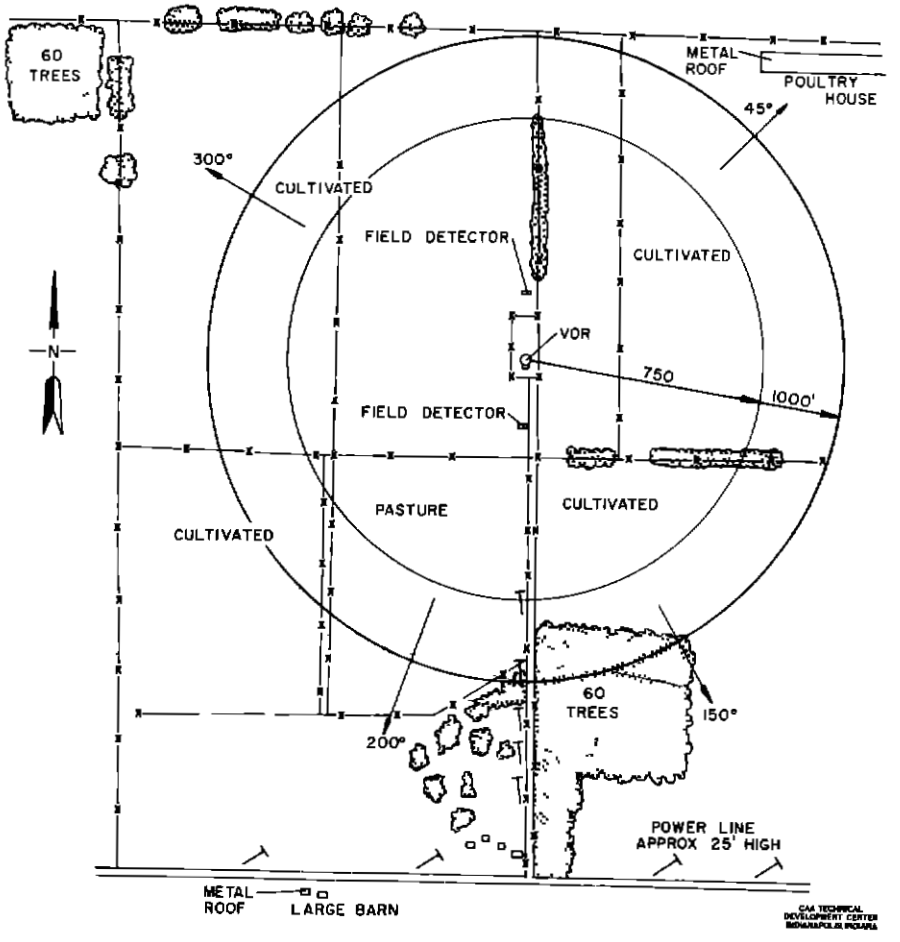

Fig 17 Map of Dayton, Ohio, VOR Site

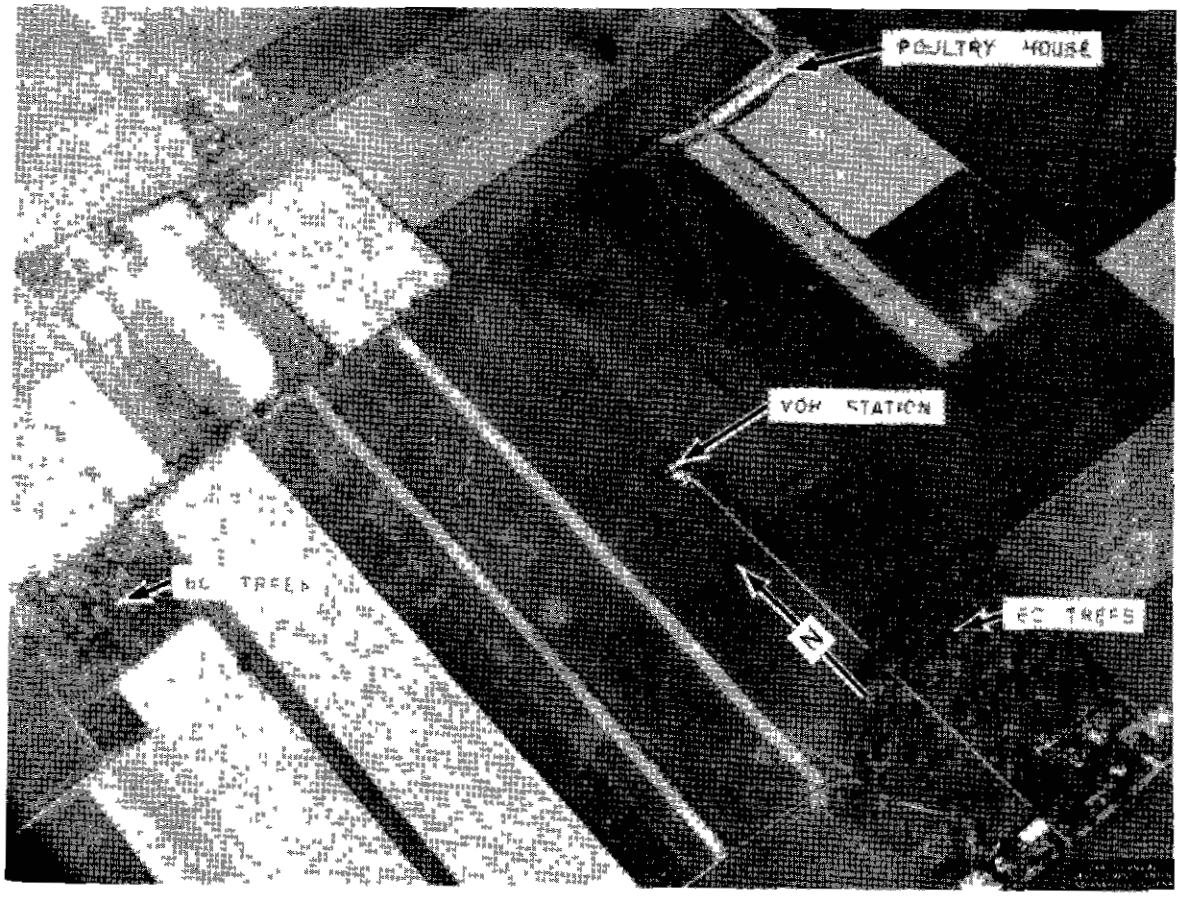

Fig 18 Aerial View of Dayton, Ohio, VOR Site

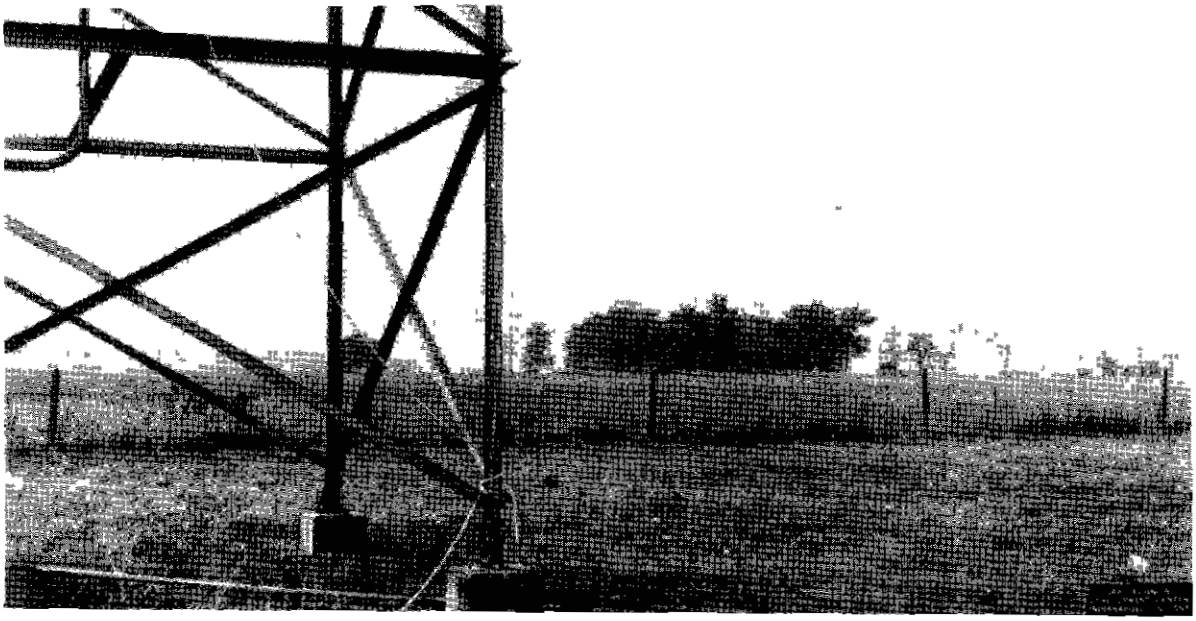

Fig 19 View of the Woods Northwest of the Dayton, Ohio, VOR

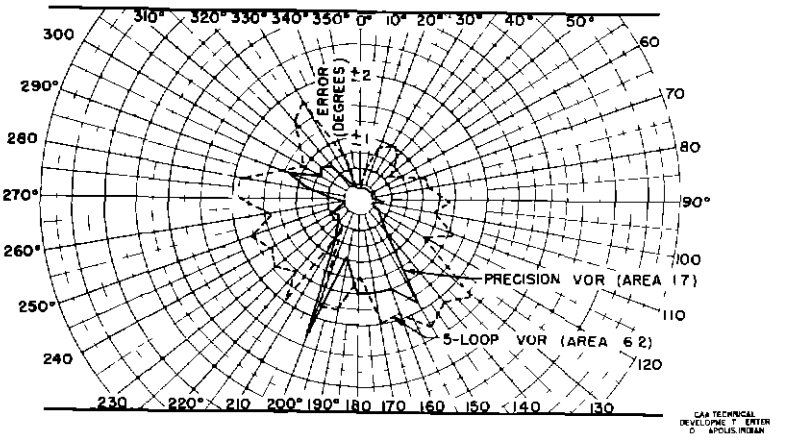

Fig 20 Plot of Course Scalloping from Measurements at the Dayton, Ohio, VOR

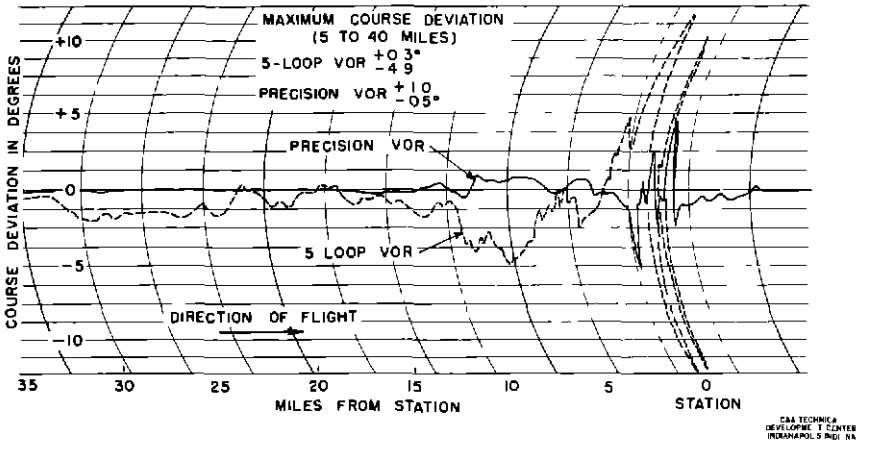

Fig 21 Course Displacement Measured on 260° Radial Flights on the 5-Loop VOR and Precision VOR

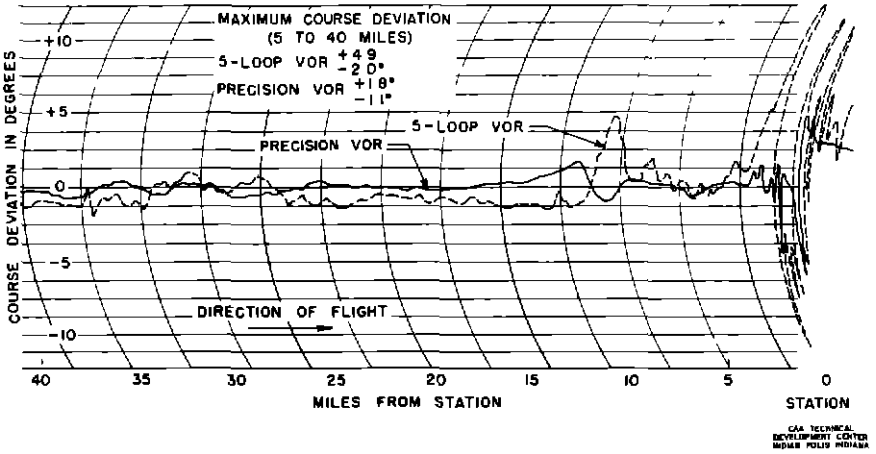

Fig 22 Course Displacement Measured on 150° Radial Flights on the 5-Loop VOR and Precision VOR

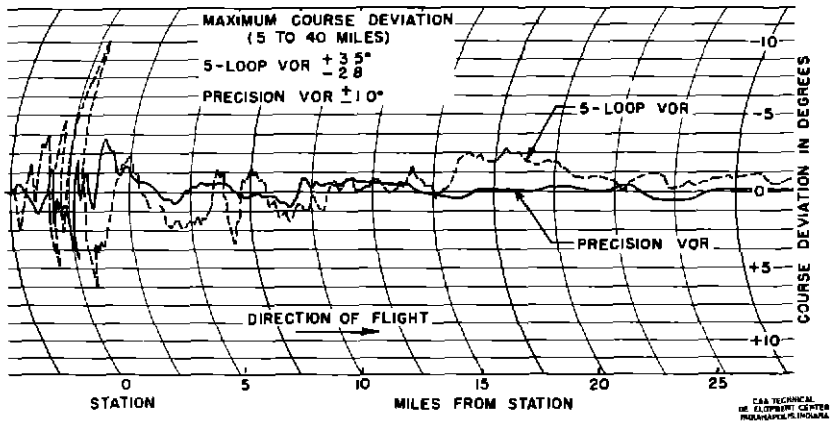

Fig 23 Course Displacement Measured on 130° Radial Flights on the 5-Loop VOR and Precision VOR

CONCLUSIONS

The results of flight tests show that the precision omnirange will provide bearing information with markedly less scalloping and siting errors than is possible with a conventional omnirange Ground tests of the precision omnirange demonstrated that accurate bearing information is an inherent characteristic of the multilobe VOR.

Measurements of siting errors show that the maximum scalloping amplitude when compared to that of a conventional VOR was reduced approximately 70 per cent when the reflecting object was a horizontal wire and 75 per cent when the reflecting object was a hangar A considerable improvement is evident when comparing scalloping areas of the precision VOR with a conventional VOR The scalloping areas were reduced by a factor of approximately 19 to 1 for a horizontal wire, 10 to 1 for hangars and vertical towers, and 3 65 to 1 for groups of large trees

Radial flights showed an improvement with respect to course bends and scalloping by a factor varying between 2 to 1 and 6 to 1 with all types of reflecting objects

The inherent ambiguity of bearings can be resolved but will require further development.

Theory predicts a marked improvement in course scalloping for a precision VOR utilizing 40 sideband elements compared with the precision VOR with 20 sideband elements The precision omnirange principle is applicable to radiating elements other than loops

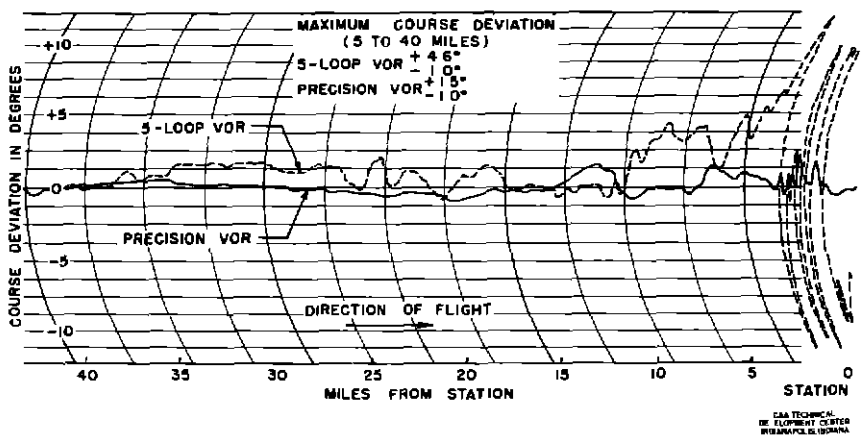

Fig 24 Course Displacement Measured on 180° Radial Flights on the 5-Loop VOR and Precision VOR